

Pseudo-zero-mode Landau levels and collective excitations in bilayer graphene

K. Shizuya

Yukawa Institute for Theoretical Physics, Kyoto University, Kyoto 606-8502, Japan

(Received 6 January 2009; published 6 April 2009)

Bilayer graphene in a magnetic field supports eight zero-energy Landau levels, which, as a tunable band gap develops, split into two nearly degenerate quartets separated by the band gap. A close look is made into the properties of such an isolated quartet of pseudo-zero-mode levels at half filling in the presence of an in-plane electric field and the Coulomb interaction, with focus on revealing further controllable features in bilayer graphene. The half-filled pseudo-zero-mode levels support, via orbital level mixing, charge carriers with nonzero electric moment, which would lead to field-induced level splitting and the current-induced quantum Hall effect. It is shown that the Coulomb interaction enhances the effect of the in-plane field and their interplay leads to rich spectra of collective excitations, pseudospin waves, accessible by microwave experiments; also a duality in the excitation spectra is revealed.

DOI: [10.1103/PhysRevB.79.165402](https://doi.org/10.1103/PhysRevB.79.165402)

PACS number(s): 73.43.-f, 71.10.Pm, 77.22.Ch

I. INTRODUCTION

Graphene, a monolayer of graphite, attracts a great deal of attention, both experimentally¹⁻³ and theoretically⁴⁻⁸ for its unusual electronic transport, characteristic of “relativistic” charge carriers—massless Dirac fermions. Dirac fermions give rise to quantum phenomena reflecting the particle-hole picture of the vacuum state, such as Klein tunneling⁹ and, especially in a magnetic field, such peculiar phenomena¹⁰⁻¹⁴ as spectral asymmetry and induced charges, which are rooted in the chiral anomaly (i.e., a quantum conflict between charge and chirality conservations). Graphene provides a special laboratory to test such consequences of quantum electrodynamics. Actually, the half-integer quantum Hall (QH) effect and the presence of the zero-energy Landau level observed^{1,2} in graphene are a manifestation of spectral asymmetry.

Bilayer graphene is equally exotic¹⁵⁻¹⁷ as monolayer graphene. It has a unique property that the band gap is controllable¹⁸⁻²² by the use of external gates or chemical doping; this makes bilayers richer in electronic properties. In bilayer graphene interlayer coupling modifies the intralayer relativistic spectra to yield quasiparticles with a parabolic energy dispersion.¹⁶ The particle-hole structure still remains in the “chiral” form of a Schrödinger Hamiltonian and there arise eight zero(-energy)-mode Landau levels (two per valley and spin) in a magnetic field.

Zero-mode Landau levels, specific to graphene, deserve attention in their own right. They would show quite unusual dielectric response^{23,24} while they carry normal Hall conductance e^2/h per level; for bilayer graphene direct calculations²⁵ indicate that the zero modes show no dielectric response for a zero band gap but the response grows linearly with the band gap. In bilayer graphene, with a tunable band gap, the zero-mode levels split into two quartets separated by the band gap at different valleys. Such an isolated quartet of “pseudo”-zero-mode levels remains nearly degenerate and, as noted earlier,²⁵ the level splitting is enhanced or controlled by an in-plane electric field or by an injected current; this opens up the possibility of the current-induced QH effect for the pseudo-zero-mode sector around half filling, i.e., at filling factor $\nu = \pm 2$.

The purpose of this paper is to further examine the properties of the pseudo-zero-mode levels, especially, coherence and collective excitations in the presence of an external field and the Coulomb interaction. The pseudo-zero-mode levels at half filling support, via orbital level mixing, charge carriers with nonzero electric dipole moment, which is responsible for field-induced level splitting and the current-induced QH effect. Along this line our discussion comes in contact with the works of Barlas *et al.*²⁶ and Abergel *et al.*²⁷ who, from the viewpoint of QH ferromagnets, studied the interaction-driven QH effect in the nearly degenerate octet of zero-mode levels in bilayer graphene. Our paper partly extends their analysis by revealing an interesting interplay between the in-plane field and Coulomb exchange interaction, which leads to rich spectra of collective excitations, accessible by microwave experiments. We shall find a duality in the excitation spectra and, under certain circumstances, an instability in pseudospin textures.

In Sec. II we briefly review some basic features of the pseudo-zero-mode levels in bilayer graphene. In Sec. III we construct a low-energy effective theory for the half-filled pseudo-zero-mode sector. In Sec. IV we examine the spectrum and collective excitations in it. In Sec. V we study the microwave response of collective excitations. Section VI is devoted to a summary and discussion.

II. BILAYER GRAPHENE

Bilayer graphene consists of two coupled hexagonal lattices of carbon atoms, arranged in Bernal $A'B$ stacking. The electron fields in it are described by four-component spinors on the four inequivalent sites (A, B) and (A', B') in the bottom and top layers, and their low-energy features are governed by the two inequivalent Fermi points K and K' in the Brillouin zone. The intralayer coupling $\gamma_0 \equiv \gamma_{AB}$ is related to the Fermi velocity $v_0 = (\sqrt{3}/2)a_L\gamma_0/\hbar \approx 10^6$ m/s (with $a_L = 0.246$ nm) in monolayer graphene. The interlayer couplings $\gamma_1 \equiv \gamma_{A'B}$ and $\gamma_3 \equiv \gamma_{AB'}$ are 1 order of magnitude weaker than γ_0 ; numerically,²⁸ $\gamma_1 \approx 0.30$ eV, $\gamma_3 \approx 0.10$ eV, and $\gamma_0 \approx 2.9$ eV.

Actually, interlayer hopping via the (A', B) dimer sites modifies the intralayer relativistic spectra to yield spectra with a quadratic dispersion and the characteristic cyclotron energy $\omega_c = 2v_0^2/(\gamma_1 \ell^2) \approx 3.9B[\text{T}] \text{ meV}$ with a magnetic field $B[\text{T}]$ in tesla. The low-energy branches, thereby, are essentially described by two-component spinors on the (A, B') sites (with the high-energy branches separated by a large gap $\sim \gamma_1$). The effective Hamiltonian is written as¹⁶

$$H = \int d^2\mathbf{x} [\psi^\dagger (\mathcal{H}_+ - eA_0) \psi + \chi^\dagger (\mathcal{H}_- - eA_0) \chi],$$

$$\mathcal{H}_\xi = \mathcal{H}_0 + \mathcal{H}_{\text{as}},$$

$$\mathcal{H}_0 = \omega_c \begin{pmatrix} & -(a^\dagger)^2 + \lambda a \\ -a^2 + \lambda a^\dagger & \end{pmatrix},$$

$$\mathcal{H}_{\text{as}} = \xi \frac{U}{2} \begin{pmatrix} 1 - za^\dagger a & \\ & -(1 - zaa^\dagger) \end{pmatrix}, \quad (2.1)$$

together with coupling to electromagnetic potentials (A_i, A_0) . Here, assuming placing graphene in a uniform magnetic field $B > 0$, we have rescaled the kinetic momenta $\Pi_i = -i\partial_i + eA_i$ with the magnetic length $\ell = 1/\sqrt{eB}$ and defined $a = \sqrt{2eB}(\Pi_x - i\Pi_y)$ and $a^\dagger = \sqrt{2eB}(\Pi_x + i\Pi_y)$, so that $[a, a^\dagger] = 1$; we set $A_i \rightarrow B(-y, 0)$ to supply a strong magnetic field B normal to the sample plane. The field $\psi = (\psi_A, \psi_{B'})^t$ refers to the K valley with $\mathcal{H}_+ = \mathcal{H}_{\xi=1}$ while $\chi = (\chi_{B'}, \chi_A)^t$ refers to the K' valley with $\mathcal{H}_- = \mathcal{H}_{\xi=-1}$. For simplicity we ignore weak Zeeman coupling and suppress the electron spin indices.

In \mathcal{H}_0 the linear kinetic term, leading to ‘‘trigonal warping,’’ represents direct interlayer hopping via γ_3 , with $\lambda = \xi(\gamma_3/\gamma_0)(\sqrt{2}v_0/\ell)/\omega_c \approx \pm 0.3/\sqrt{B[\text{T}]}$. \mathcal{H}_{as} takes into account a possible layer asymmetry, caused by an interlayer voltage ΔA_0 , which leads to a tunable^{18–20} gap $U \approx e\Delta A_0$ between the conduction and valence bands. The $O(za^\dagger a)$ terms in \mathcal{H}_{as} represent a kinetic asymmetry related to the charge depleted from the dimer sites; note that it is very weak with $z = 2\omega_c/\gamma_1 \approx 0.026B[\text{T}] \ll 1$.

While the linear spectra are lost, the bilayer Hamiltonian still possesses a key feature of relativistic field theory, the particle-hole (or chiral) structure of the quantum vacuum: when the tiny $O(zU)$ asymmetry is ignored, the spectrum of \mathcal{H}_ξ , in general, is symmetric about zero energy $\epsilon = 0$, apart from possible $\epsilon = \pm U/2$ spectra that evolve from the zero-energy modes of \mathcal{H}_0 . Indeed, for $\lambda = 0$ the spectrum of \mathcal{H}_ξ consists of an infinite tower of Landau levels $|n, y_0\rangle$ of paired positive and negative energies,

$$\epsilon_n = s_n \omega_c \sqrt{|n|(|n| - 1) + (U/2\omega_c)^2} - \frac{1}{4}\xi z U, \quad (2.2)$$

labeled by integers $n = \pm 2, \pm 3, \dots$ and p_x (or $y_0 \equiv \ell^2 p_x$); $s_n \equiv \text{sgn}\{n\} = \pm 1$ specifies the sign of ϵ_n .

In addition, there arise nearly degenerate Landau levels carrying the orbital index $|n|=0$ and $|n|=1$ with spectrum

$$\epsilon_{|n|=0} = \xi U/2, \quad \epsilon_{|n|=1} = \xi(U/2)(1 - z). \quad (2.3)$$

From now on we take, without loss of generality, $U > 0$ and denote $n=0_\pm$ and $n = \pm 1$ to specify these pseudo-zero-mode levels. There are four such pseudo-zero-mode levels (or two levels per spin) at each valley and they reside on different layers; the $(0_+, 1)$ quartet on A sites at $\xi=1$ valley is separated from the $(0_-, -1)$ quartet on B' sites by a band gap U . Each quartet remains degenerate, apart from $O(zU)$ fine splitting.

The presence of the pseudo-zero-mode levels and their doublefold degeneracy (per spin and valley) both have a topological origin and are consequences of spectral asymmetry, or the nonzero index of the Hamiltonian $\mathcal{H}_\xi|_{U \rightarrow 0}$,

$$\text{Index}[\mathcal{H}_\xi|_{U \rightarrow 0}] = \int d^2\mathbf{x} 2(eB/2\pi), \quad (2.4)$$

which is tied to the chiral anomaly in 1+1 dimensions. This degeneracy is unaffected by the presence of trigonal warping $\lambda \neq 0$ alone²⁵ but is affected by nontrivial diagonal components in \mathcal{H}_ξ . Indeed, the kinetic asymmetry $\sim za^\dagger a$ leads to tiny level splitting and an electric field $\sim \partial_t A_0$ can also enhance the splitting. In other words, the pseudo-zero-mode levels have an intrinsic tendency to be degenerate, but this at the same time implies that their fine structure or the way they get mixed depends sensitively on the environment.

The main purpose of the present paper is to study such controllable features of the isolated pseudo-zero-mode quartet in the presence of external fields and Coulomb interactions. We are particularly interested in the properties of such a quartet at half filling, where mixing of the zero modes leads to nontrivial coherence effects and collective excitations. For definiteness we focus on the $n=(0_+, 1)$ sector at $\xi=1$ valley, i.e., around filling factor $\nu=2$ (or $\nu=1$ when the spin is resolved) and ignore the presence of other levels which are separated by relatively large gaps; the $\nu=-2$ case is treated likewise. We ignore the effect of trigonal warping, which causes only a negligibly small level splitting²⁵ of $O(z\lambda^4) < 1/10^3$, apart from a common level shift of $O(z\lambda^2)$.

To project out the $n=(0_+, 1)$ sector let us make the Landau-level structure explicit by the expansion $\psi(\mathbf{x}, t) = \sum_{n, y_0} \langle \mathbf{x} | n, y_0 \rangle \psi_n(y_0, t)$ with the field operators obeying $\{\psi_m(y_0, t), \psi_n^\dagger(y_0, t)\} = \delta_{mn} \delta(y_0 - y_0')$. The charge density $\rho_{-\mathbf{p}}(t) = \int d^2\mathbf{x} e^{i\mathbf{p}\cdot\mathbf{x}} \psi^\dagger \psi$ is thereby written as

$$\rho_{-\mathbf{p}} = \gamma_{\mathbf{p}} \sum_{k, n=-\infty}^{\infty} g_{kn}(\mathbf{p}) \int dy_0 \psi_k^\dagger e^{i\mathbf{p}\cdot\mathbf{r}} \psi_n, \quad (2.5)$$

where $\gamma_{\mathbf{p}} = e^{-\ell^2 \mathbf{p}^2/4}$; $\mathbf{r} = (r_x, r_y) = (i\ell^2 \partial/\partial y_0, y_0)$ stands for the center coordinate with uncertainty $[r_x, r_y] = i\ell^2$. For the $(0_+, 1)$ sector the relevant coefficients are given by²⁵ $g_{00}(\mathbf{p}) = 1$, $g_{11}(\mathbf{p}) = 1 - \ell^2 \mathbf{p}^2/2$, $g_{10}(\mathbf{p}) = i\ell p/\sqrt{2}$, and $g_{01}(\mathbf{p}) = i\ell p^\dagger/\sqrt{2}$ with $p \equiv p_y + ip_x$.

Let us put the $\psi_{0_\pm}(y_0, t)$ and $\psi_1(y_0, t)$ modes into a two-component spinor $\Psi = (\psi_{0_+}, \psi_1)^t$ and define the pseudospin operators in the $(0_+, 1)$ orbital space,

$$S_{-\mathbf{p}}^\mu = \gamma_{\mathbf{p}} \int dy_0 \Psi^\dagger \frac{1}{2} \sigma^\mu e^{i\mathbf{p}\cdot\mathbf{r}} \Psi, \quad (2.6)$$

where $\sigma^\mu = (1, \sigma^a)$ ($\mu=0\sim 3$) with Pauli matrices σ^a and $\sigma^0=1$. The charge density $\rho_{-\mathbf{p}}$ projected to the $(0_+, 1)$ sector is thereby written as

$$\bar{\rho}_{-\mathbf{p}} = 2(w_{\mathbf{p}}^0 S_{-\mathbf{p}}^0 + w_{\mathbf{p}}^3 S_{-\mathbf{p}}^3 + w_{\mathbf{p}}^1 S_{-\mathbf{p}}^1 + w_{\mathbf{p}}^2 S_{-\mathbf{p}}^2), \quad (2.7)$$

where $w_{\mathbf{p}}^0 = 1 - \ell^2 \mathbf{p}^2/4$, $w_{\mathbf{p}}^3 = \ell^2 \mathbf{p}^2/4$, $w_{\mathbf{p}}^1 = i\ell p_y/\sqrt{2}$, and $w_{\mathbf{p}}^2(\mathbf{p}) = i\ell p_x/\sqrt{2}$. Note that $(S_{-\mathbf{p}}^2, S_{-\mathbf{p}}^1)^t$ acts as a vector under rotations about the z axis $\parallel B$.

The Hamiltonian H of Eq. (2.1) is projected into the $(0_+, 1)$ sector to yield

$$\Delta \bar{H} = - \int d^2 \mathbf{x} e A_0 \bar{\rho} + \int dy_0 m \Psi^\dagger \sigma^3 \Psi, \quad (2.8)$$

where $m \equiv zU/4$; the common energy shift $(1-z/2)U/2$ of the $(0_+, 1)$ sector has been isolated from $\Delta \bar{H}$. One can equally write $\Delta \bar{H}$ as

$$\Delta \bar{H} = 2 \sum_{\mathbf{p}} \mathcal{P}_{\mathbf{p}}^\mu S_{-\mathbf{p}}^\mu \quad (2.9)$$

with $\mathcal{P}_{\mathbf{p}}^\mu$ being the Fourier transform of $\mathcal{P}^\mu(\mathbf{x}, t)$,

$$\begin{aligned} \mathcal{P}^0 &= -m - eA_0 - \frac{1}{4} e \ell^2 \nabla \cdot \mathbf{E}, \\ \mathcal{P}^3 &= m - \frac{1}{4} e \ell^2 \nabla \cdot \mathbf{E}, \\ (\mathcal{P}^2, \mathcal{P}^1) &= \frac{e\ell}{\sqrt{2}} (E_x, E_y), \end{aligned} \quad (2.10)$$

where $\mathbf{E}_{\parallel} = (E_x, E_y) = -\partial_x A_0$ denotes the in-plane electric field.

The Coulomb interaction also simplifies via projection. The pseudo-zero-modes at each valley essentially lie on the same layer, apart from a negligibly small admixture of $O(\omega_c/\gamma_1) \sim 10^{-3}$. One may thus retain only the intralayer interaction for Ψ ,

$$\bar{H}^C = \frac{1}{2} \sum_{\mathbf{p}} v_{\mathbf{p}} \bar{\rho}_{-\mathbf{p}} \bar{\rho}_{\mathbf{p}}, \quad (2.11)$$

where $v_{\mathbf{p}} = 2\pi\alpha/(\epsilon_b |\mathbf{p}|)$ is the Coulomb potential with the fine-structure constant $\alpha = e^2/(4\pi\epsilon_0) \approx 1/137$ and the substrate dielectric constant ϵ_b ; $\sum_{\mathbf{p}} = \int d^2 \mathbf{p}/(2\pi)^2$. The normal-ordered charges in \bar{H}^C are rewritten as

$$\begin{aligned} \bar{\rho}_{-\mathbf{p}} \bar{\rho}_{\mathbf{p}} &= \bar{\rho}_{-\mathbf{p}} \bar{\rho}_{\mathbf{p}} - \Delta, \\ \Delta &= 2\gamma_{\mathbf{p}}^2 \{ |w_{\mathbf{p}}^\mu|^2 S_{\mathbf{p}}^0 + 2w_{\mathbf{p}}^0 w_{\mathbf{p}}^3 S_{\mathbf{p}}^3 \} \end{aligned} \quad (2.12)$$

under a symmetric integration over \mathbf{p} .

The pseudospin operators $S_{\mathbf{p}}^\mu$ obey the $SU(2) \times W_\infty$ algebra,^{29,30}

$$[S_{\mathbf{p}}^a, S_{\mathbf{k}}^b] = c(p, k) i \epsilon^{abc} S_{\mathbf{p}+\mathbf{k}}^c - is(p, k) \delta^{ab} S_{\mathbf{p}+\mathbf{k}}^0,$$

$$[S_{\mathbf{p}}^0, S_{\mathbf{k}}^0] = -is(p, k) S_{\mathbf{p}+\mathbf{k}}^0,$$

$$[S_{\mathbf{p}}^0, S_{\mathbf{k}}^a] = [S_{\mathbf{p}}^a, S_{\mathbf{k}}^0] = -is(p, k) S_{\mathbf{p}+\mathbf{k}}^a, \quad (2.13)$$

where (a, b) runs over 1–3, and

$$s(p, k) = \sin\left(\frac{\ell^2 \mathbf{p} \times \mathbf{k}}{2}\right) e^{\ell^2 \mathbf{p} \cdot \mathbf{k}/2}. \quad (2.14)$$

$\mathbf{p} \times \mathbf{k} \equiv \epsilon^{ij} p_i k_j = p_x k_y - p_y k_x$; for $c(p, k)$ set $\sin(\cdots) \rightarrow \cos(\cdots)$ in $s(p, k)$.

III. PSEUDOSPIN TEXTURES

In this section we study the properties of the pseudo-zero-mode levels at half filling using the projected Hamiltonian $\bar{H} \equiv \Delta \bar{H} + \bar{H}^C$ and the charge algebra (2.13), with focus on orbital mixing of the zero modes. Let us suppose that such a half-filled state is given by a classical configuration where the pseudospin points in a fixed direction in pseudospin space, i.e., $S_{\mathbf{p}=\mathbf{0}}^a = \frac{1}{2} N_e n^a$ and $n^a n^a = 1$ with the total number of electrons $N_e = 2S_{\mathbf{p}=\mathbf{0}}^0$.

Note that $n^3 = 1$ corresponds to the filled $n=0_+$ level with the vacant $n=1$ level while $n^3 = -1$ represents the filled $n=1$ level. The direction $\mathbf{n} = (n^1, n^2, n^3)$ would, in general, vary in response to the external field A_0 , and, as \mathbf{n} tilts from $n^3 = \pm 1$, the $n=0_+$ and $n=1$ levels start to mix. For self-consistency we assume that A_0 represents a uniform in-plane electric field $\mathbf{E}_{\parallel} = -\partial_x A_0$ and that it leads to a homogeneous state $|G\rangle$ of uniform density $\rho_0 = \nu/(2\pi\ell^2)$ (with filling factor $\nu=2$ for the spin-degenerate $\nu=2$ state or $\nu=1$ for the spin-resolved $\nu=1$ state). We thus consider all classical configurations with $\langle G | S_{\mathbf{p}=\mathbf{0}}^a | G \rangle = \frac{1}{2} N_e n^a$ and single out the ground state or the associated n^a by minimizing the energy $\langle G | \bar{H} | G \rangle$. For n^a we use the parametrization $n^1 = \sin \theta \cos \phi$, $n^2 = \sin \theta \sin \phi$, and $n^3 = \cos \theta$ with $-\pi < \theta \leq \pi$ and $0 \leq \phi \leq \pi$. We denote expectation values $\langle G | \mathcal{O} | G \rangle \equiv \langle \mathcal{O} \rangle$ for short.

Let us first substitute the charge and pseudospin, $\langle S_{\mathbf{p}}^0 \rangle = \frac{1}{2} \rho_0 \delta_{\mathbf{p}, \mathbf{0}}$ and $\langle S_{\mathbf{p}}^a \rangle = \frac{1}{2} \rho_0 n^a \delta_{\mathbf{p}, \mathbf{0}}$, into $\Delta \bar{H}$. [Here $\delta_{\mathbf{p}, \mathbf{0}} = (2\pi)^2 \delta^2(\mathbf{p})$, and $\delta_{\mathbf{0}, \mathbf{0}} = \int d^2 \mathbf{x}$ equals the total area, so that $N_e = \rho_0 \delta_{\mathbf{0}, \mathbf{0}}$.] This yields the response of the classical state $|G\rangle$ to an external probe, $\langle \Delta \bar{H} \rangle = \rho_0 \int d^2 \mathbf{x} n^\mu \mathcal{P}^\mu$ with

$$n^\mu \mathcal{P}^\mu = -eA_0 + m(\cos \theta - 1) - \mathbf{E}_{\parallel} \cdot \mathbf{d}_e,$$

$$\mathbf{d}_e = -\frac{e\ell}{\sqrt{2}} (n^2, n^1) = -\frac{e\ell}{\sqrt{2}} \sin \theta \hat{\mathbf{n}}_{\parallel}, \quad (3.1)$$

where $\hat{\mathbf{n}}_{\parallel} = (\hat{n}_x, \hat{n}_y) = (\sin \phi, \cos \phi)$ is an in-plane unit vector.

Note that the half-filled pseudo-zero-mode state has an in-plane electric dipole moment \mathbf{d}_e of strength $(e\ell/\sqrt{2})|\sin \theta|$ per electron, proportional to the in-plane component (n^2, n^1) of the pseudospin. Mixing of the $n=0_+$ and $n=1$ modes gives rise to this dipole and its in-plane direction $\hat{\mathbf{n}}_{\parallel}$ is related to the relative phase between them; i.e., under $U(1)$ transformations $\Psi = (\psi_0, \psi_1)^t \rightarrow e^{-i\phi_{\text{rel}}\sigma^3/2} \Psi$, $\hat{\mathbf{n}}_{\parallel}$ rotates,

$$(S^1 + iS^2) \rightarrow e^{i\phi_{\text{rel}}}(S^1 + iS^2) \text{ or } \phi \rightarrow \phi + \phi_{\text{rel}}. \quad (3.2)$$

This tells us that a change in relative phase caused by a change in direction of the dipole is physically observable.

In the absence of the Coulomb interaction, n^a naturally points in the $-\mathcal{P}^a$ direction and, as a result, an in-plane field, coupled to the electric dipole, works to enhance the pseudo-zero-mode level splitting,²⁵

$$\Delta\epsilon = 2\sqrt{m^2 + e^2\ell^2\mathbf{E}_\parallel^2/2}. \quad (3.3)$$

We shall discuss below how the Coulomb interaction modifies this.

The calculation of the Coulomb energy $\langle G|\bar{H}^C|G\rangle \equiv \langle \bar{H}^C \rangle$ requires the knowledge of pseudospin structure factors $\langle G|S_{\mathbf{p}}^\mu S_{\mathbf{q}}^\nu|G\rangle \equiv \langle S_{\mathbf{p}}^\mu S_{\mathbf{q}}^\nu \rangle$, which, for the present half-filled state with pseudospin $\propto n^a$, are given by

$$\langle S_{\mathbf{p}}^\mu S_{\mathbf{q}}^\nu \rangle = \frac{1}{4}\rho_0[s^{\mu\nu}\gamma_{\mathbf{p}}^2\delta_{\mathbf{p}+\mathbf{q},\mathbf{0}} + n^\mu n^\nu \rho_0\delta_{\mathbf{p},\mathbf{0}}\delta_{\mathbf{q},\mathbf{0}}], \quad (3.4)$$

where μ and ν run from 0 to 3 with $n^0=1$ and $\{n^a\} = (n^1, n^2, n^3)$; $(s^{\mu\nu})^\dagger = s^{\nu\mu}$ with $s^{\mu 0}=0$ and

$$\begin{aligned} s^{33} &= \sin^2 \theta, \\ s^{11} &= \cos^2 \theta \cos^2 \phi + \sin^2 \phi, \\ s^{22} &= \cos^2 \theta \sin^2 \phi + \cos^2 \phi, \\ s^{31} &= -\sin \theta \cos \theta \cos \phi + i \sin \theta \sin \phi, \\ s^{32} &= -\sin \theta \cos \theta \sin \phi - i \sin \theta \cos \phi, \\ s^{12} &= -\sin^2 \theta \sin \phi \cos \phi + i \cos \theta \cos 2\phi. \end{aligned} \quad (3.5)$$

See Appendix A for details. Actually, the normal-ordered correlation functions take simpler form

$$\langle :S_{\mathbf{p}}^\mu S_{\mathbf{q}}^\nu: \rangle = -\frac{1}{4}\rho_0 n^\mu n^\nu (\gamma_{\mathbf{p}}^2\delta_{\mathbf{p}+\mathbf{q},\mathbf{0}} - \rho_0\delta_{\mathbf{p},\mathbf{0}}\delta_{\mathbf{q},\mathbf{0}}) \quad (3.6)$$

with which one can cast the Coulomb energy in the form

$$\langle \bar{H}^C \rangle = -\frac{1}{2}N_e \sum_{\mathbf{p}} v_{\mathbf{p}} e^{-q^2/2} C_\theta(q^2/4), \quad (3.7)$$

where $q^2 \equiv \ell^2 \mathbf{p}^2$ and $C_\theta(x) = 1 - x(1-x)(1 - \cos \theta)^2$. From $\langle \bar{H}^C \rangle$ we have omitted a constant $(N_e/2)\rho_0 v_{\mathbf{p}=\mathbf{0}}$ which is removed when the neutralizing positive background is taken into account. Integrating over \mathbf{p} yields a typical scale of the Coulomb exchange energy,

$$V_1 = \sum_{\mathbf{p}} v_{\mathbf{p}} e^{-\ell^2 \mathbf{p}^2/2} = \frac{\alpha}{\epsilon_b \ell} \sqrt{\frac{\pi}{2}}, \quad (3.8)$$

The effective Hamiltonian $H_{\text{eff}} = \langle \Delta \bar{H} + \bar{H}^C \rangle$ is conveniently written in \mathbf{x} space as $H_{\text{eff}} = \rho_0 \int d^2 \mathbf{x} \mathcal{H}_{\text{eff}}$ with

$$\mathcal{H}_{\text{eff}} = -eA_0 + E(\theta),$$

$$E(\theta) = -\frac{1}{2}V_1 + m(\cos \theta - 1) + \mathcal{E} \sin \theta + \frac{1}{32}V_1(1 - \cos \theta)^2, \quad (3.9)$$

where $\mathcal{E} = (e\ell/\sqrt{2})\mathbf{E}_\parallel \cdot \hat{\mathbf{n}}_\parallel$. In the present notation (with $\rho_0 \int d^2 \mathbf{x} \rightarrow N_e$) \mathcal{H}_{eff} stands for energy per electron in state $|G\rangle$ with pseudospin $\propto \mathbf{n}$. The Coulomb correlation energy $\propto V_1$ consists of a negative uniform component $-V_1/2$ [relative to the zero of energy $(U/2)(1-z/2)$] and a polarization-dependent component which alone favors $\theta=0$, i.e., the filled $n=0_+$ level, and which varies continuously by an amount $\Delta E_c = (1/8)V_1$ as \mathbf{n} sweeps in pseudospin space. The Coulomb interaction thus significantly enhances the pseudo-zero-mode level splitting.

The stable configuration of the half-filled zero-mode state $|G\rangle$ is determined by minimizing $E(\theta)$ with respect to \mathbf{n} or (θ, ϕ) . Obviously $E(\theta)$ depends on ϕ through \mathcal{E} , which attains a maximum when $\mathbf{n}_\parallel \parallel \mathbf{E}_\parallel$ or $\mathcal{E} = e\ell|\mathbf{E}_\parallel|/\sqrt{2}$. Accordingly it is convenient, without loss of generality, to suppose that the in-plane field \mathbf{E}_\parallel and \mathbf{n}_\parallel lie along the y axis, $\mathcal{E} = e\ell E_y/\sqrt{2} \geq 0$, and $\phi=0$. With this choice the “1,” “2,” and “3” axes in pseudospin space coincide with the y , x , and $-z$ axes in real space, respectively. We adopt this choice and set $(n^1, n^2, n^3) = (\sin \theta, 0, \cos \theta)$ in what follows.

One can now look for possible ground-state configurations by writing down a phase diagram as a function of m and \mathbf{E}_\parallel . For clarity of exposition we leave it for a later stage and here study collective excitations over a given ground state $|G\rangle|_{\mathbf{n}}$. We focus on a special class of low-energy collective excitations, pseudospin waves, which are rotations about the energy minimum $|G\rangle|_{\mathbf{n}}$ in pseudospin space.

As is familiar from the case of quantum Hall ferromagnets,³⁰ such a collective state is represented as a texture state

$$|\tilde{G}\rangle = e^{-i\mathcal{O}}|G\rangle|_{\mathbf{n}}, \quad (3.10)$$

where the operator $e^{-i\mathcal{O}}$ with

$$\mathcal{O} = \sum_{\mathbf{p}} \gamma_{\mathbf{p}}^{-1} \Omega_{\mathbf{p}}^a S_{\mathbf{p}}^a \quad (3.11)$$

locally tilts the pseudospin from \mathbf{n} to $\tilde{\mathbf{n}}_{\mathbf{p}}$ by small angle $\Omega_{\mathbf{p}} \sim \mathbf{n} \times \tilde{\mathbf{n}}_{\mathbf{p}}$. Repeated use of the charge algebra (2.13) then allows one to express the texture-state energy $\langle \tilde{G}|\bar{H}|\tilde{G}\rangle = \langle G|e^{i\mathcal{O}}\bar{H}e^{-i\mathcal{O}}|G\rangle$ in terms of the structure factors in Eq. (3.4), and this yields an effective Hamiltonian as a functional of $\Omega_{\mathbf{p}}^a$ or its \mathbf{x} -space representative $\Omega^a(\mathbf{x}, t)$.

The angle variables $\Omega^a(\mathbf{x}, t)$ may be normalized, so that $\sum_a (\Omega^a)^2 = 1$ classically. As we shall see below, the effective theory is expressed in terms of the following components of Ω^a :

$$\begin{aligned} \eta &\equiv \Omega^1 \cos \theta - \Omega^3 \sin \theta, \\ \zeta &\equiv \Omega^2 \end{aligned} \quad (3.12)$$

along the two orthogonal axes (i.e., the tilted 1 axis and the 2 axis) perpendicular to the pseudospin \mathbf{n} with normalization $(n^a \Omega^a)^2 + \eta^2 + \zeta^2 = 1$. [Here we have chosen $\phi=0$ and set $\{n^a\} = (\sin \theta, 0, \cos \theta)$, as remarked above; the $\phi \neq 0$ case, if

needed, is readily recovered.^{31]} Actually they refer to the following induced pseudospin components in the excited state $|\tilde{G}\rangle$:

$$\begin{aligned}\eta &\sim -\gamma_{\mathbf{p}}^{-1}\langle\tilde{G}|S^2|\tilde{G}\rangle, \\ \xi &\sim \gamma_{\mathbf{p}}^{-1}\langle\tilde{G}|S^1\cos\theta - S^3\sin\theta|\tilde{G}\rangle,\end{aligned}\quad (3.13)$$

as seen from the induced pseudospin $\delta\langle\tilde{G}|S_{\mathbf{p}}^a|\tilde{G}\rangle \approx (\rho_0/2)\gamma_{\mathbf{p}}\epsilon^{abc}\Omega_{\mathbf{p}}^b n^c$.

We expand $\langle\tilde{G}|\bar{H}|\tilde{G}\rangle$ to second order in Ω and retain all powers of derivatives acting on Ω to study the spectrum over a wide range of wavelengths. The calculation is outlined in Appendix B. The result is

$$\begin{aligned}\langle\tilde{G}|\bar{H}|\tilde{G}\rangle &= \rho_0 \int d^2\mathbf{x} (\mathcal{H}_{\text{eff}} + \mathcal{H}_{\text{coll}}), \\ \mathcal{H}_{\text{coll}} &= \frac{1}{2}\eta\Gamma_{\eta}\eta + \frac{1}{2}\xi\Gamma_{\xi}\xi + \xi W_{\mathbf{p}}\eta + \mathcal{H}_{\text{ch}} + \delta\mathcal{H}, \\ \Gamma_{\eta} &= -\mathcal{E}/\sin\theta + F_{\mathbf{p}}, \\ \Gamma_{\xi} &= E'(\theta) + G_{\mathbf{p}}, \\ \delta\mathcal{H} &= E'(\theta)\{\xi + \Omega^1\eta/(2\sin\theta)\},\end{aligned}\quad (3.14)$$

$E'(\theta) = dE(\theta)/d\theta$, etc. Here

$$\begin{aligned}F_{\mathbf{p}} &= \frac{V_c}{2}\left[\frac{1}{2}\sqrt{\frac{\pi}{2}} + \xi_q + P_{-}\lambda_q\right], \\ G_{\mathbf{p}} &= \frac{V_c}{2}\left[\frac{1}{2}\sqrt{\frac{\pi}{2}} + \xi_q - b_q\sin^2\theta - P_{-}\lambda_q\cos^2\theta\right], \\ W_{\mathbf{p}} &= -\frac{V_c}{2}\left[2\frac{p_x p_y}{\mathbf{p}^2}\lambda_q\cos\theta + i\frac{\ell p_x}{\sqrt{2}}\tau_q\sin\theta\right]\end{aligned}\quad (3.15)$$

with $V_c = \alpha/(\epsilon_b\ell)$, $P_{-} = (p_x^2 - p_y^2)/\mathbf{p}^2$, and

$$\begin{aligned}\xi_q &= \nu e^{-q^2/2}\frac{q}{2} - \int_0^{\infty} dz e^{-z^2/2}\left(1 - \frac{1}{2}z^2\right)J_0(zq), \\ \lambda_q &= \nu e^{-q^2/2}\frac{q}{2} - \frac{1}{2}\int_0^{\infty} dz e^{-z^2/2}z^2J_2(zq), \\ b_q &= \nu e^{-q^2/2}(q/2 - q^3/8) + \frac{1}{8}\int_0^{\infty} dz e^{-z^2/2}(1 - 4z^2 + z^4)J_0(zq), \\ \tau_q &= \nu e^{-q^2/2}q/2 + \frac{2}{q}\int_0^{\infty} dz e^{-z^2/2}z\left(1 - \frac{1}{4}z^2\right)J'_0(zq),\end{aligned}\quad (3.16)$$

where $q = \ell|\mathbf{p}|$; substitution $\mathbf{p} \rightarrow -i\nabla$ is understood in the \mathbf{x} representation. For $\mathbf{p} \rightarrow 0$, $\xi_q \rightarrow -(1/2)\sqrt{\pi}/2$, $(\lambda_q, b_q) \rightarrow 0$,

and $\tau_q \rightarrow -(1/4)\sqrt{\pi}/2$ while they all tend to zero for $\mathbf{p} \rightarrow \infty$. See Appendix C for more explicit forms of the integrals involved in these functions.

In $\mathcal{H}_{\text{coll}}$, \mathcal{H}_{ch} refers to a topological charge (to be detected with a constant potential A_0)

$$\rho_0 \int d^2\mathbf{x} \mathcal{H}_{\text{ch}} = -e \int d^2\mathbf{x} A_0 \frac{\nu}{8\pi} \epsilon^{abc} \epsilon^{ij} (\partial_i \Omega^a) (\partial_j \Omega^b) n^c, \quad (3.17)$$

where $\epsilon^{xy} = 1$ and $\epsilon^{123} = 1$. With n^c promoted to Ω^c , $\int d^2\mathbf{x} \mathcal{H}_{\text{ch}}$ involves the winding number, which implies³⁰ that possible topologically nontrivial semiclassical excitations (skyrmions) associated with Ω^a , in general, carry electric charge of integral multiples of νe . Note also that $\delta\mathcal{H}$, involving a term linear in ξ , disappears for a stable-state configuration for which $E'(\theta) = 0$.

The kinetic term for Ω^a is supplied from the electron kinetic term as Berry's phase,

$$\langle\tilde{G}|i\partial_t|\tilde{G}\rangle = -\frac{1}{4}\rho_0 \sum_{\mathbf{k}} n^c \epsilon^{abc} \Omega_{-\mathbf{k}}^a \partial_t \Omega_{\mathbf{k}}^b = \frac{\rho_0}{2} \int d^2\mathbf{x} \xi \partial_t \eta \quad (3.18)$$

to $O(\Omega\Omega)$, apart from surface terms. This shows that ξ is canonically conjugate to $(\rho_0/2)\eta$. One can now write the effective Lagrangian for the collective excitations as

$$L = \frac{1}{2}\xi \partial_t \eta - \mathcal{H}_{\text{coll}}[\eta, \xi]. \quad (3.19)$$

Note here that this Lagrangian is written as

$$\rho_0 \int d^2\mathbf{x} L = \langle G | e^{iO} (i\partial_t - \bar{H}) e^{-iO} | G \rangle. \quad (3.20)$$

This representation realizes and systematizes the single-mode approximation (SMA) (Ref. 29) within a variational framework.³² The present theory thus embodies nonperturbative aspects of the SMA.

Upon elimination of ξ , Eq. (3.19) leads to an alternative form of the effective Lagrangian for η as follows:

$$\begin{aligned}L_{\Phi} &= \frac{1}{2}(\partial_t \Phi)^2 - \frac{1}{2}\Phi(M_{\mathbf{p}})^2\Phi, \\ M_{\mathbf{p}} &= 2\sqrt{\Gamma_{\eta}\Gamma_{\xi} - |W_{\mathbf{p}}|^2},\end{aligned}\quad (3.21)$$

where we have set $\Phi = (1/2)(\Gamma_{\xi})^{-1/2}\eta$.

The spectrum $M_{\mathbf{p}}$ of collective excitations is in general anisotropic in \mathbf{p} at low energies and depends critically on the stable-state configuration \mathbf{n} . In particular, the leading long-wavelength correction in $\mathcal{H}_{\text{coll}}$ starts with the direct Coulomb interaction of $O(\mathbf{p})$, which leads to the spectrum,

$$M_{\mathbf{p}} \approx \sqrt{(2\kappa_{\eta}\kappa_{\xi})^2 + V_c \frac{\nu\ell}{|\mathbf{p}|} \{\kappa_{\eta}^2 \cos^2\theta p_y^2 + \kappa_{\xi}^2 p_x^2\}},$$

$$\kappa_{\eta}^2 \equiv \Gamma_{\eta}|_{\mathbf{p}=0} = -\mathcal{E}/\sin\theta,$$

$$\kappa_\zeta^2 \equiv \Gamma_\zeta|_{\mathbf{p}=0} = E''(\theta). \quad (3.22)$$

The excitation gap at zero wave vector is thus given by $M_{\mathbf{p}=0} = 2\kappa_\eta\kappa_\zeta$. In contrast, $M_{\mathbf{p}}$ recovers isotropy and the standard excitonic behavior³³ at short wavelengths,

$$M_{\mathbf{p}\rightarrow\infty} \approx V_1/2 + \kappa_\eta^2 + \kappa_\zeta^2 \quad (3.23)$$

with $\Gamma_\eta \rightarrow V_1/4 + \kappa_\eta^2$, $\Gamma_\zeta \rightarrow V_1/4 + \kappa_\zeta^2$, and $W_{\mathbf{p}} \rightarrow 0$ for $\mathbf{p} \rightarrow \infty$; $V_1 = V_c \sqrt{\pi}/2$.

It is worth noting here that the Coulomb interaction alone yields $\kappa_\eta^2 = 0$, i.e., a flat direction in (η, ζ) space. This implies that, unlike in ordinary bilayer QH systems, there is no cost of interlayer capacitance energy for the pseudo-zero-mode sector which essentially resides in the same layer. Coherence is thus easier to form in this sector of bilayer graphene.

If we set $\theta \rightarrow 0$, our $M_{\mathbf{p}}$ precisely reproduces the excitation spectrum derived in Ref. 26 by assuming spatial isotropy; actually, the effective Hamiltonian of Ref. 26 is apparently different from our $\mathcal{H}_{\text{coll}}$ but the spectrum turns out to be the same. It is our use of general textures \mathbf{n} that allows $\mathcal{H}_{\text{coll}}$ to handle spatially anisotropic situations as well.

IV. POSSIBLE GROUND STATES AND COLLECTIVE EXCITATIONS OVER THEM

In this section we study the spectrum of the half-filled pseudo-zero-mode state and the associated collective excitations. Let us first gain a rough idea of the strengths of m and \mathbf{E}_\parallel relative to the Coulomb correlation energy ΔE_c . A naive estimate

$$\Delta E_c = \frac{1}{8} \sqrt{\frac{\pi}{2}} \frac{\alpha}{\epsilon_b \ell} \approx 2.2 \sqrt{B[\text{T}]} \text{ meV} \quad (4.1)$$

with a typical value $\epsilon_b \sim 4$ indicates that the bare Coulomb interaction is apparently sizable, as compared with the basic Landau gap $\omega_c \approx 3.9B[\text{T}] \text{ meV}$. We remark that Eq. (4.1) is likely to overestimate ΔE_c . Actually ΔE_c is written as an integral of the form

$$\Delta E_c \sim 2 \sum_{\mathbf{p}} v_{\mathbf{p}} e^{-q^2/2} (q^2/4)(1 - q^2/4) \quad (4.2)$$

with $q = \ell|\mathbf{p}|$, and the main contribution comes from the momentum region $|\mathbf{p}|\ell \sim 1$, where the Coulomb interaction is very efficiently weakened [$v_{\mathbf{p}} \rightarrow v_{\mathbf{p}}/\epsilon(\mathbf{p})$], as indicated by a random-phase-approximation study²⁵ of the dielectric function $\epsilon(\mathbf{p})$. This screening effect essentially comes from vacuum (Dirac-sea) polarization, specific to graphene. It may effectively be taken care of by setting $\epsilon_b \rightarrow \epsilon_b \epsilon_{\text{sc}}$; a simple estimate³⁴ gives $\epsilon_{\text{sc}} \sim 9$ at $B \sim 1 \text{ T}$ and $\epsilon_{\text{sc}} \sim 3.6$ at $B \sim 10 \text{ T}$.

The ratio of the intrinsic zero-mode level gap $2m = 0.013B[\text{T}]U$ to ΔE_c is generally small,

$$m/\Delta E_c \approx 3\epsilon_{\text{sc}} \times 10^{-3} \sqrt{B[\text{T}]} U[\text{meV}], \quad (4.3)$$

for a band gap U of $O(1 \text{ meV})$ and increases with B and U . For the in-plane field $\mathcal{E} = e\ell|\mathbf{E}_\parallel|/\sqrt{2}$ the ratio

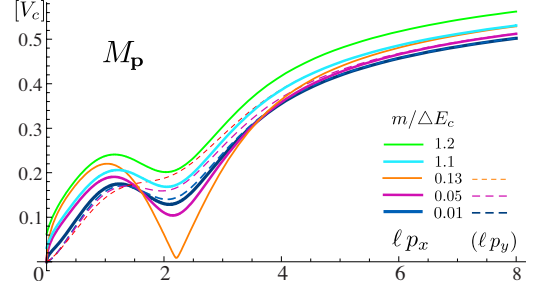


FIG. 1. (Color online) Excitation spectra $M_{\mathbf{p}}$ plotted in units of $V_c = \alpha/\epsilon_b \ell$ for $m/\Delta E_c = 0.01, 0.05, 0.13, 1.1,$ and 1.2 . The real curves refer to the profiles in p_x at $p_y = 0$ (i.e., normal to the in-plane field E_y) and dashed curves to those in p_y at $p_x = 0$.

$$\mathcal{E}/\Delta E_c \approx 0.9\epsilon_{\text{sc}} \times 10^{-3} E[\text{V/cm}]/B[\text{T}] \quad (4.4)$$

is on the order of 10% for $E = |\mathbf{E}_\parallel| = 10 \text{ V/cm}$ at $B = 1 \text{ T}$ with $\epsilon_{\text{sc}} \sim 9$. Note that $\mathcal{E} \approx m$ for $\mathcal{E} \approx 3.6 \text{ V/cm} \times U[\text{meV}]B[\text{T}]^{3/2}$.

To determine the orbital configuration of the half-filled zero-mode state $|G\rangle$ one has to look for the minimum of $E(\theta)$, $E_{\text{min}} = E(\theta_{\text{min}})$ with $E'(\theta_{\text{min}}) = 0$. Let us begin with the case where \mathbf{E}_\parallel is absent. It is clear from $E(\theta)$ of Eq. (3.9) that the Coulomb correlation favors $\theta = 0$ while the intrinsic asymmetry $m > 0$ alone favors $\theta = \pi$; ΔE_c and m thus compete.

(i) In case $m > \Delta E_c$ (although rather unrealistic), one finds $E_{\text{min}} = -(2m - \Delta E_c)$ and $\kappa_\eta^2 = \kappa_\zeta^2 = m - \Delta E_c$ at $\theta = \pi$. The collective excitations have a finite energy gap $M_{\mathbf{p}=0} = 2(m - \Delta E_c) > 0$ and the spectrum is isotropic, reflecting the rotational invariance of the bilayer system about the z axis $\parallel B$ or, more explicitly, invariance of $\Delta \bar{H} + \bar{H}^C$ (for $A_0 = 0$) under $U(1)$ rotations in Eq. (3.2).

(ii) On the other hand, for $0 < m < \Delta E_c$, one finds $E_{\text{min}} = -\Delta E_c (m/\Delta E_c)^2$ at $\theta = \pm \theta_{\text{min}}$ with $\sin^2(\theta_{\text{min}}/2) = m/\Delta E_c$; θ_{min} varies from 0 to π with increasing m . Here we encounter a somewhat strange situation. Note that, for $\theta \neq 0, \pm \pi$, the rotational invariance is spontaneously broken. Indeed, one finds $\kappa_\eta^2 = 0$ and $\kappa_\zeta^2 = 2m(1 - m/\Delta E_c)$. Accordingly the collective excitations about this state are gapless (as the Nambu-Goldstone modes), and spectrum (3.22) is anisotropic in \mathbf{p} .

The excitation spectrum $M_{\mathbf{p}}$ in general exhibits a local minimum (roton minimum) around $|\mathbf{p}|\ell \sim 2$ [see Fig. 1(a)]. In the $0 < m < \Delta E_c$ range of case (ii), the roton minimum changes critically with m : the minimum in p_x comes down, as m is increased from zero, and touches zero (gap) at $m/\Delta E_c \approx 0.131$ (with $\theta_{\text{min}} \approx 42.6^\circ$). The spectrum loses sense (becoming pure imaginary) until m reaches $m/\Delta E_c \approx 0.869$ (with $\theta_{\text{min}} \approx 137.4^\circ$) where the roton minimum reappears; it then rises and returns to the $m = 0$ spectrum at $m = \Delta E_c$. This peculiar feature inspires one to find an interesting structure of $E(\theta)$,

$$E(\theta; m) = E(\pi - \theta; \Delta E_c - m), \quad (4.5)$$

valid for $\mathcal{E} \neq 0$ as well. This implies that the half-filled state realized at θ_{min} for a given $m < \Delta E_c/2$ is paired with the state realized with angle $\pi - \theta_{\text{min}}$ at a larger intrinsic gap $\propto m' = \Delta E_c - m$. Both the energy $E(\theta_{\text{min}})$ and excitation spectrum

$M_{\mathbf{p}}$ completely agree for this pair of states, as seen from Eqs. (3.15) and (3.21). In particular, the filled $n=0$ level realized at $m=0$ and the filled $n=1$ level realized at $m=\Delta E_c$ share the same energy and collective excitations. We thus find a kind of (small- m /large- m) duality in the $0 \leq m \leq \Delta E_c$ range.

In this m range the texture state, taken to be homogeneous in space, acquires spontaneous in-plane electric polarization $\propto \sin \theta_{\min}$. The anomalous behavior of the roton spectrum about $m/\Delta E_c \sim 0.5$ or $\theta \sim \pi/2$, mentioned above, reflects a potential instability of the texture state due to spontaneous polarization. Such electrically polarized *homogeneous* configurations, unless polarization is relatively weak, are unstable against local charge inhomogeneities and would decay into *inhomogeneous* configurations.

A local charge excess would align electric dipoles outward or inward and let them drift in a magnetic field. One may thus imagine a picture of charged electric dipoles drifting around local charge centers (distributed randomly or in some patterns on the real sample and substrate), clockwise or anticlockwise depending on the sign of the local excess charge. We speculate that the half-filled state in the realistic $0 < m < \Delta E_c$ range may form many such domains for stabilization.

Let us next set $m \rightarrow 0$, i.e., consider the case of zero band gap $U=0$ and study the effect of \mathbf{E}_{\parallel} . The in-plane field $\mathcal{E} = e\ell E_y / \sqrt{2} > 0$ tilts the pseudospin toward $\theta = -\pi/2$ and competes with ΔE_c which favors $\theta=0$. As a result, θ_{\min} varies from 0 to $-\pi/2$ as E_y is increased. The charge carriers thereby acquire a nonzero electric dipole moment $\propto \sin \theta$ and the pseudospin waves always have a finite excitation gap for $\mathcal{E} \neq 0$ (see Fig. 2). For weak field $4\mathcal{E}/\Delta E_c \equiv R \ll 1$, one finds $\theta_{\min} \approx -R^{1/3}$, $E_{\min} \approx -(3/16)R^{4/3}\Delta E_c$, and $\kappa_{\zeta}^2 \approx 3\kappa_{\eta}^2 \approx (3/4)R^{2/3}\Delta E_c$, so that the excitation gap grows as

$$M_{\mathbf{p}=0} \approx (\sqrt{3}/2)(4\mathcal{E}/\Delta E_c)^{2/3}\Delta E_c. \quad (4.6)$$

For larger $\mathcal{E} \gg \Delta E_c$ the gap rises almost linearly with \mathcal{E} ,

$$M_{\mathbf{p}=0} \approx 2\mathcal{E} + \Delta E_c/2, \quad (4.7)$$

along with $\kappa_{\eta}^2 \approx \mathcal{E}$ and $\kappa_{\zeta}^2 \approx \mathcal{E} + \Delta E_c/2$. As seen from Fig. 2, Eqs. (4.6) and (4.7) combine to give a practically good description of the excitation gap over the entire range of \mathcal{E} ; crossover takes place around $\mathcal{E}/\Delta E_c \sim 0.3$. Note that the Coulomb correction significantly enhances the excitation gap; in particular, the gap rises prominently as $\mathcal{E}^{2/3}$ for a weak field.

For $\mathcal{E} \neq 0$ the excitation spectrum $M_{\mathbf{p}}$ is necessarily anisotropic, especially at low momenta, and, as seen from a contour plot of $M_{\mathbf{p}}$ in Fig. 3, anisotropy of the roton minima already develops around $\mathcal{E}/\Delta E_c \sim 0.02$. The spectrum recovers isotropy for $|\mathbf{p}|\ell \sim 5$ or larger and the asymptotic spectrum is lifted roughly by the amount of the excitation gap, as seen from the spectrum profiles in Fig. 3(a) and from Eq. (3.23). Note that the roton minimum, unlike the $m \neq 0$ case, shows no sign of instability.

When both m and \mathcal{E} are present, their effects generally tend to add up. The texture excitations always have a gap and their potential instability, in a certain range about $m/\Delta E_c \sim 0.5$, weakens and eventually disappears with increasing \mathcal{E} ;

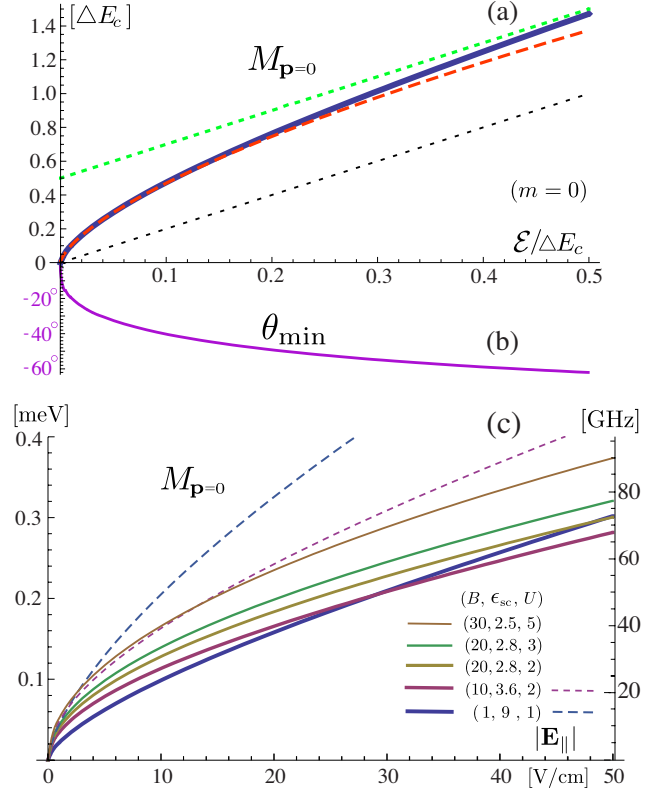


FIG. 2. (Color online) (a) Excitation gap at zero momentum plotted in units of ΔE_c as a function of the in-plane field $\mathcal{E}/\Delta E_c$. The red dashed curve refers to Eq. (4.6) and the green dotted line to the asymptotic form of Eq. (4.7). (b) Angle of inclination θ_{\min} in degrees. (c) Excitation gap $M_{\mathbf{p}=0}$, in units of meV and GHz, plotted as a function of the in-plane field $|\mathbf{E}_{\parallel}|$ for some typical values of $(B[\text{T}], \epsilon_{sc}, U[\text{meV}])$. Dashed curves refer to the cases where the screening effect is turned off, $\epsilon_{sc} \rightarrow 1$.

the roton dip remains to be a local minimum as long as $\mathcal{E} > m$. We remark that the duality implied by Eq. (4.5) would hold in the presence of \mathcal{E} as well.

In Fig. 2(c) we plot the excitation gap as a function of $|\mathbf{E}_{\parallel}|$ for some typical values of $B[\text{T}]$ and $m \propto U[\text{meV}]$. With the effect of screening ϵ_{sc} taken into account, $M_{\mathbf{p}=0}$ falls in roughly the same frequency range of microwaves.

If \mathbf{E}_{\parallel} is sufficiently strong, a sizable excitation gap $M_{\mathbf{p}=0}$ would arise, leading to an incompressible $\nu=2$ state. One could thereby observe the (spin-degenerate) $\nu=2$ Hall plateau with a suitably strong injected current for $U \neq 0$ and $U=0$ as well.

Of the pseudospin $\propto \mathbf{n}$ the angle θ is related to the ratio in amplitude of the $n=0_+$ and $n=1$ modes while the angle ϕ is related to the relative phase between them. One would now have control of mixing of the zero-mode levels by adiabatically changing the strength and direction of an injected current.

V. CURRENT AND RESPONSE

In this section we study the response of the pseudospin waves in the $(0_+, 1)$ sector under uniform fields B and E_y to

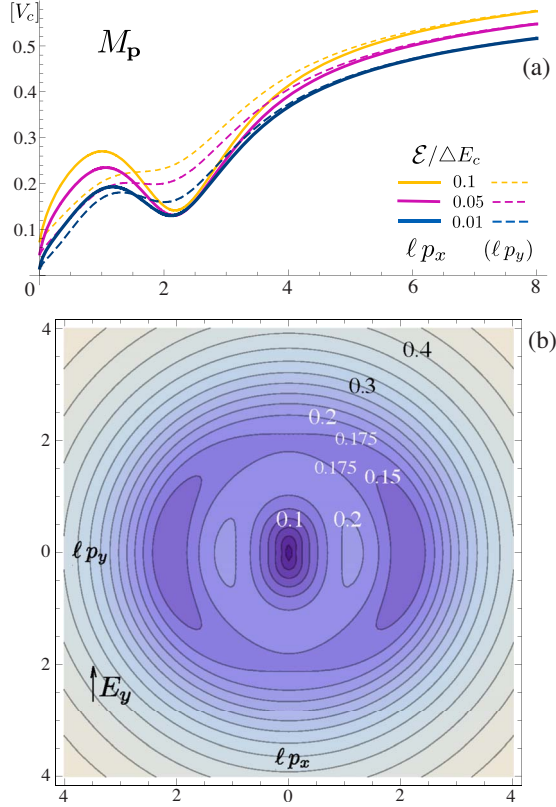


FIG. 3. (Color online) (a) Excitation spectra $M_{\mathbf{p}}$, in units of $V_c = \alpha/\epsilon_b \ell$, for $\mathcal{E}/\Delta E_c = 0.01, 0.05$, and 0.1 . The real curves refer to the profiles in p_x and dashed curves to those in p_y . (b) Contour plot of $M_{\mathbf{p}}$ for $\mathcal{E}/\Delta E_c = 0.02$.

a weak time-varying external field. To this end we consider a weak vector potential $\mathbf{A}(t) = (A_x, A_y)$, which describes an external field $\sim \partial_t \mathbf{A}$ and, at the same time, serves to probe the current. For simplicity we take it to be spatially uniform.

The current operator $\delta H/\delta \mathbf{A}$ derives from two parts in H of Eq. (2.1). One coming from \mathcal{H}_0 is the ordinary form of current, which has no projection to the $(0_+, 1)$ sector and induces transitions to other levels. The other one, specific to bilayer graphene, derives from the $O(zU)$ part of \mathcal{H}_{as} , and the relevant $O(\mathbf{A})$ portion of its $(0_+, 1)$ projection is written as

$$\bar{H}_A = -2\sqrt{2}m\rho_0 e\ell(A_x S_{\mathbf{p}=\mathbf{0}}^1 - A_y S_{\mathbf{p}=\mathbf{0}}^2), \quad (5.1)$$

where $m = zU/4$. Evaluating $\langle \tilde{G} | \bar{H}_A | \tilde{G} \rangle$ yields an addition to $\mathcal{H}_{\text{coll}}$ of the form

$$\mathcal{H}_A = -\sqrt{2}e\ell\{c_0 A_x + c_x A_x \zeta + c_y A_y \eta\},$$

$$c_0 = m \sin \theta, \quad c_x = m \cos \theta, \quad c_y = m. \quad (5.2)$$

One might read from \mathcal{H}_A the current density carried by the zero-mode sector as $j_x^{\text{zm}} = -\sqrt{2}\rho_0 e\ell m \sin \theta_{\min}$ [which, for $V_c = 0$, equals $-(ve^2/h)E_y$]. This, unfortunately, is not a complete amount of current yet. Inter-Landau-level transitions caused by the ordinary current induce some extra charge in the $(0_+, 1)$ sector. In other words, the presence of \mathbf{A} causes level mixing, which modifies the current within the $(0_+, 1)$ sector. Such a modification was calculated earlier³² for stan-

dard QH systems and, in the present case, it is given by

$$\delta \bar{\rho}_{-\mathbf{p}} \approx (S_{-\mathbf{p}}^0 - S_{-\mathbf{p}}^3)u_{11}(\mathbf{p}),$$

$$u_{11}(\mathbf{p}) \approx 2ie\ell^2(1 - \ell^2 \mathbf{p}^2/4)(p_x A_y - p_y A_x) \quad (5.3)$$

to $O(\mathbf{A})$, apart from terms of $O(\partial_t A_i/\omega_c)$. This $u_{11}(\mathbf{p})$ represents charge accumulated in the $n=1$ level via the $n=1 \rightarrow \pm 2 \rightarrow 1$ inter-Landau-level transitions.

The induced charge also carries current within the $(0_+, 1)$ sector via the interaction

$$\delta \bar{H}_A = \frac{1}{2} \sum_{\mathbf{p}} v_{\mathbf{p}} \cdot \{\bar{\rho}_{\mathbf{p}}, \delta \bar{\rho}_{-\mathbf{p}}\} - \sum_{\mathbf{p}} e(A_0)_{\mathbf{p}} \delta \bar{\rho}_{-\mathbf{p}}. \quad (5.4)$$

The current response is now calculated from $\langle \tilde{G} | \bar{H}_A + \delta \bar{H}_A | \tilde{G} \rangle$. The result again takes the form of Eq. (5.2) with coefficients (c_0, c_x, c_y) modified as follows:

$$c_0 = m \sin \theta + (1 - \cos \theta)\mathcal{E} + (V_1/32)\sin 2\theta$$

$$= \mathcal{E} - E'(\theta), \quad (5.5)$$

$$c_x = m \cos \theta + \dots = -E''(\theta), \quad (5.6)$$

$$c_y = m + (V_1/16)(\cos \theta - 1)$$

$$= \mathcal{E} \cos \theta / \sin \theta - E'(\theta) / \sin \theta. \quad (5.7)$$

With $E'(\theta) \rightarrow 0$, Eq. (5.5) verifies that the pseudo-zero-mode sector carries the *correct* amount of Hall current (in response to a uniform field \mathcal{E}) with conductance $\sigma_{xy} = -ve^2/h$.

The Hamiltonian $\bar{H}_A + \delta \bar{H}_A$ governs the microwave response of the pseudo-zero-mode sector. It is combined with $\mathcal{H}_{\text{coll}}$ to yield the source term $\Phi\{2c_y(\Gamma_{\zeta})^{1/2}A_y - c_x(\Gamma_{\zeta})^{-1/2}\partial_t A_x\}$ for L_{Φ} in Eq. (3.21). Solving for the stationary action then yields a response of the form $\sim A_y(\dots)\partial_t A_x$. From this one can read off the optical Hall conductance due to virtual transitions within the $(0_+, 1)$ sector,

$$\Delta\sigma_{xy}(\omega) = -\frac{ve^2}{2\pi\hbar} \cos \theta_{\min} \frac{M_0^2}{M_0^2 - \omega^2}, \quad (5.8)$$

which is significantly peaked around $\omega \sim M_0 \equiv M_{\mathbf{p}=0}$, the pseudospin-wave gap.

The collective excitations within the $(0, 1)$ sector thus contribute the $\cos \theta$ portion $[\Delta\sigma_{xy}(\omega \rightarrow 0)]$ of the Hall conductance σ_{xy} while the remaining $(1 - \cos \theta)$ portion of σ_{xy} essentially comes from the $n=1 \rightarrow \pm 2 \rightarrow 1$ virtual transitions with larger gaps $\sim \sqrt{2}\omega_c \gg M_0$. These two components are distinguishable via microwave or light response.

With disorder taken into account, the diagonal conductivity $\Delta\sigma_{xx}(\omega)$ also is significantly peaked around $\omega \sim M_0$ and M_0 varies critically with \mathcal{E} or by an injected current, as we have seen in Fig. 2. Microwave or infrared experiment,³⁵ via absorption, reflection, or conductance fluctuation, would provide a direct means to explore such unique dynamics of the pseudo-zero-modes.

VI. SUMMARY AND DISCUSSION

Zero-mode Landau levels, specific to graphene in a magnetic field, are very special. Their presence has a topological

origin in the chiral anomaly. They show quite unusual dielectric response that reflects quantum fluctuations of the vacuum state (the Dirac sea). Bilayer graphene supports eight such zero-mode levels which, unlike in monolayer graphene, involve two different orbital indices $n=0,1$. As a tunable band gap develops, four of them at one valley are isolated from the others at another valley and remain nearly degenerate although its fine structure sensitively depends, via mixing of zero modes, on the environment.

In this paper we have studied the effects of an external field and the Coulomb interaction on such an isolated zero-mode quartet. This pseudo-zero-mode sector, especially at half filling, supports, via orbital mixing, quasiparticles with charge and electric dipole, which give rise to characteristic collective excitations, pseudospin waves. We have constructed a low-energy effective theory of pseudospin waves with general pseudospin textures and noted a duality [Eq. (4.5)] in the excitation spectrum. The excitation gap at zero momentum turns out to be generally small, reflecting the intrinsic degeneracy of the pseudo-zero-mode sector, and the Coulomb exchange energy works to enhance the effect of the in-plane field on the gap. This means that the gap is tunable by an in-plane field or by an injected current; the mixing of the zero modes (i.e., relative phase and magnitude) is also externally controllable to some extent.

The pseudo-zero-mode sector of bilayer graphene is particularly suited for exploring coherence phenomena. This is because it essentially resides on the same layer so that, unlike in ordinary bilayer QH systems, there is no cost of interlayer capacitance energy for it.

An experimental signature of the field-induced gap is to observe the quantum Hall effect with an injected current; one would be able to resolve the $\nu=\pm 2$ Hall plateaus (or the spin-resolved $\nu=\pm 1$ plateaus) using a suitably strong current.

The collective excitations within the pseudo-zero-mode sector also carry a considerable portion of the total current. A direct study of the excitation gap $M_{\mathbf{p}=0}$ and its field dependence by microwave absorption or reflection would clarify the unique controllable features of the pseudo-zero-mode sector in bilayer graphene and, in addition, the effect of screening on the Coulomb correlation energy ΔE_c due to vacuum polarization.

ACKNOWLEDGMENTS

The author wishes to thank T. Morinari for useful discussions. This work was supported in part by a Grant-in-Aid for Scientific Research from the Ministry of Education, Science, Sports and Culture of Japan (Grant No. 17540253).

APPENDIX A: STATIC STRUCTURE FACTORS

In this appendix we outline the derivation of the pseudospin static structure factors $\langle S_{\mathbf{p}}^a S_{\mathbf{q}}^b \rangle$ [in Eq. (3.4)] for the half-filled pseudo-zero-mode levels $|G\rangle$ with $\langle S_{\mathbf{0}}^a \rangle = (N_e/2)n^a$ pointing in a general direction $\mathbf{n}=\{n^a\}$ in pseudospin space. Let us first note that, when only the $n=0_+$ level is filled, i.e., for $n^3=1$ polarization, these structure factors are readily cal-

culated: filling the $n=0_+$ level and leaving the $n=1$ level empty immediately imply that $\langle S_{\mathbf{p}}^{\mu} S_{\mathbf{q}}^{\nu} \rangle = (\rho_0/2)^2 \delta_{\mathbf{p},\mathbf{0}} \delta_{\mathbf{q},\mathbf{0}}$ for $\mu, \nu \in (0,3)$ and $\langle :S_{\mathbf{p}}^a S_{\mathbf{q}}^b: \rangle = 0$ for $a, b \in (1,2)$. One may then note the algebraic relation

$$S_{\mathbf{p}}^a S_{\mathbf{q}}^b = e^{f_{\mathbf{p}\mathbf{q}}} \frac{1}{2} (\delta^{ab} S_{\mathbf{p}+\mathbf{q}}^0 + i \epsilon^{abc} S_{\mathbf{p}+\mathbf{q}}^c) + :S_{\mathbf{p}}^a S_{\mathbf{q}}^b: \quad (\text{A1})$$

with $f_{\mathbf{p}\mathbf{q}} = \ell^2 (\mathbf{p} \cdot \mathbf{q} - i \mathbf{p} \times \mathbf{q})/2$ and determine, e.g., $\langle :S_{\mathbf{p}}^3 S_{-\mathbf{p}}^3: \rangle = (N_e/4)(\rho_0 \delta_{\mathbf{p},\mathbf{0}} - \gamma_{\mathbf{p}}^2)$ and $\langle S_{\mathbf{p}}^1 S_{-\mathbf{p}}^1 \rangle = (N_e/4) \gamma_{\mathbf{p}}^2$ with $\gamma_{\mathbf{p}} = e^{-\ell^2 \mathbf{p}^2/4}$.

The structure factors for the half-filled state with a general pseudospin polarization \mathbf{n} are obtained from these $n^3=1$ structure factors by a suitable rotation in pseudospin space. Note first that the $n^3=\sigma^3=\pm 1$ eigenspinors $|\pm 1\rangle$ of the Pauli matrix σ^3 are rotated by angle (θ, ϕ) to form the $\sigma^a=\pm n^a$ eigenspinors $U|\pm 1\rangle$ with $U=e^{-i\phi\sigma^3/2}e^{-i\theta\sigma^2/2}$. Accordingly we decompose the zero-mode field $\Psi=(\psi_{0+}, \psi_1)'$ [defined in Eq. (2.6)] into the $\sigma^a=\pm n^a$ eigenmodes Ψ' by writing $\Psi=U\Psi'$.

On substitution $\Psi=U\Psi'$, $S_{\mathbf{p}}^a$ are rewritten as linear combinations of the pseudospin operators $S_{\mathbf{p}}^{\prime a} \sim \Psi'^{\dagger}(\sigma^a/2)e^{i\mathbf{p}\cdot\mathbf{r}}\Psi'$ composed of Ψ' ; $S_{\mathbf{p}}^0=S_{\mathbf{p}}^{\prime 0}$. One can then calculate $\langle S_{\mathbf{p}}^{\mu} S_{\mathbf{q}}^{\nu} \rangle$ for general n^a from the structure factors $\langle S_{\mathbf{p}}^{\prime \mu} S_{\mathbf{q}}^{\prime \nu} \rangle$ for the $n^3=1$ state. The result is summarized in Eq. (3.4).

Note, in particular, that $S_{\mathbf{p}}^a = n^a S_{\mathbf{p}}^{\prime 3} + \dots$. This yields $\langle S_{\mathbf{p}}^a \rangle = n^a \langle S_{\mathbf{p}}^{\prime 3} \rangle = n^a (\rho_0/2) \delta_{\mathbf{p},\mathbf{0}}$ and tells us that the normal-ordered factors take particularly simple form $\langle :S_{\mathbf{p}}^a S_{\mathbf{q}}^b: \rangle = n^a n^b \langle :S_{\mathbf{p}}^{\prime 3} S_{\mathbf{q}}^{\prime 3}: \rangle$ or

$$\langle :S_{\mathbf{p}}^{\mu} S_{-\mathbf{p}}^{\nu}: \rangle = -n^{\mu} n^{\nu} (N_e/4) (\gamma_{\mathbf{p}}^2 - \rho_0 \delta_{\mathbf{p},\mathbf{0}}) \quad (\text{A2})$$

with $n^0=1$, as quoted in Eq. (3.6).

APPENDIX B: COLLECTIVE EXCITATIONS

In this appendix we outline the derivation of $\mathcal{H}_{\text{coll}}$ in Eq. (3.14). Let us first consider the contribution from the Coulomb interaction $\frac{1}{2} \sum_{\mathbf{p}} v_{\mathbf{p}} J_{\mathbf{p}}$ with $J_{\mathbf{p}} = \langle G | (\bar{\rho}_{\mathbf{p}})^{\mathcal{O}} (\bar{\rho}_{-\mathbf{p}})^{\mathcal{O}} | G \rangle$ and $(\bar{\rho}_{\mathbf{p}})^{\mathcal{O}} = e^{i\mathcal{O}} \bar{\rho}_{\mathbf{p}} e^{-i\mathcal{O}}$. Expanding $(\bar{\rho}_{\mathbf{p}})^{\mathcal{O}}$ in powers of $\mathcal{O} \propto \Omega$ by repeated use of the W_{∞} algebra (2.13) and subsequently substituting the structure factors in Eq. (3.4) allow one to evaluate $J_{\mathbf{p}}$. The $O(\Omega)$ term is thereby written as

$$\begin{aligned} J_{\mathbf{p}}^{(1)} &= -\rho_0 \gamma_{\mathbf{p}}^2 \Omega_{\mathbf{k}=\mathbf{0}}^a \epsilon^{abc} w_{\mathbf{p}}^b w_{-\mathbf{p}}^{\beta} s^{\{c,\beta\}} \\ &= \rho_0 \gamma_{\mathbf{p}}^2 \Omega_{\mathbf{0}}^2 (|w_{\mathbf{p}}^1|^2 - |w_{\mathbf{p}}^3|^2) s^{\{1,3\}} \end{aligned} \quad (\text{B1})$$

under a symmetric integration over \mathbf{p} ; $s^{\{c,\beta\}} \equiv s^{c\beta} + s^{\beta c}$ for short. (Here, we have employed the convention $\phi=0$ and $n^2=0$, as remarked in the text.)

Similarly, the $O(\Omega \Omega)$ term is written as

$$\begin{aligned}
J_{\mathbf{p}}^{(2)} &= \rho_0^2 \gamma_{\mathbf{p}}^2 |\epsilon^{abc} n^a w_{\mathbf{p}}^b \Omega_{-\mathbf{p}}^c|^2 + \frac{\rho_0}{2} \gamma_{\mathbf{p}}^2 \sum_{\mathbf{k}} \cos^2 \left(\frac{1}{2} \ell^2 \mathbf{k} \times \mathbf{p} \right) \\
&\times (N_1 + N_2) + \frac{\rho_0}{2} \gamma_{\mathbf{p}}^2 \sum_{\mathbf{k}} \sin^2 \left(\frac{1}{2} \ell^2 \mathbf{k} \times \mathbf{p} \right) (N_3 + N_4) \\
&- \frac{\rho_0}{4} \gamma_{\mathbf{p}}^2 \sum_{\mathbf{k}} \sin(\ell^2 \mathbf{k} \times \mathbf{p}) (2N_5 + N_6) \quad (\text{B2})
\end{aligned}$$

with

$$\begin{aligned}
N_1 &= \Omega_{-\mathbf{k}}^\alpha \Omega_{\mathbf{k}}^a w_{\mathbf{p}}^\beta w_{\mathbf{p}}^b \epsilon^{\alpha\beta\gamma} \epsilon^{abc} s^{\{\gamma,c\}}, \\
N_2 &= -\Omega_{-\mathbf{k}}^\alpha \Omega_{\mathbf{k}}^a w_{\mathbf{p}}^\beta w_{\mathbf{p}}^\beta \epsilon^{abj} \epsilon^{\alpha c j} s^{\{c,\beta\}}, \\
N_3 &= \Omega_{-\mathbf{k}}^\alpha \Omega_{\mathbf{k}}^a |w_{\mathbf{p}}^0|^2 s^{\{\alpha,a\}}, \\
N_4 &= -\Omega_{-\mathbf{k}}^\alpha \Omega_{\mathbf{k}}^a w_{\mathbf{p}}^\beta w_{\mathbf{p}}^\beta s^{\{\alpha,\beta\}}, \\
N_5 &= \Omega_{-\mathbf{k}}^\alpha \Omega_{\mathbf{k}}^a w_{\mathbf{p}}^0 w_{\mathbf{p}}^\beta \epsilon^{\alpha\beta\gamma} s^{\{\gamma,a\}}, \\
N_6 &= \Omega_{-\mathbf{k}}^a \Omega_{\mathbf{k}}^b \epsilon^{abc} w_{\mathbf{p}}^0 w_{\mathbf{p}}^\beta s^{\{c,\beta\}}, \quad (\text{B3})
\end{aligned}$$

where $\mathbf{k} \times \mathbf{p} = k_x p_y - k_y p_x$.

One can evaluate $\sum_{\mathbf{p}} v_{\mathbf{p}} J_{\mathbf{p}}$ by integrating over \mathbf{p} and leaving the \mathbf{k} integration as it is. One may express the sines and cosines in terms of $e^{\pm i \ell^2 \mathbf{p} \times \mathbf{k}}$. Integration over \mathbf{p} is then carried out as a Fourier transform of the form $\sum_{\mathbf{p}} v_{\mathbf{p}} e^{-\ell^2 \mathbf{p}^2/2 + i \mathbf{p} \cdot \mathbf{x}}$ (powers of p_i) with $\mathbf{x} \rightarrow \ell^2 (\times \mathbf{k}) \equiv \ell^2 (k_y, -k_x)$.

The rest of terms in $\mathcal{H}_{\text{coll}}$ are obtained via the induced pseudospin to $O(\Omega\Omega)$,

$$\begin{aligned}
\langle \langle S_{\mathbf{p}}^a \rangle \rangle &= \frac{\rho_0}{2} \gamma_{\mathbf{p}} \left[n^a \delta_{\mathbf{p},0} + \epsilon^{abc} \Omega_{\mathbf{p}}^b n^c - \frac{1}{2} \{n^a (\Omega^b, \Omega^b)_{\mathbf{p}} \right. \\
&\quad \left. - (\Omega^a, \Omega^b)_{\mathbf{p}} n^b \right], \quad (\text{B4})
\end{aligned}$$

where $(\Omega^a, \Omega^b)_{\mathbf{p}} \equiv \sum_{\mathbf{k}} \cos(\ell^2 \mathbf{k} \times \mathbf{p}/2) \Omega_{-\mathbf{k}+\mathbf{p}}^a \Omega_{\mathbf{k}}^b$ for short. This, in particular, is used to evaluate the contribution $\langle \Delta^{\mathcal{O}} \rangle$ from Δ in Eq. (2.12). Somewhat tedious calculations along these lines eventually lead to $\mathcal{H}_{\text{coll}}$ in Eq. (3.14).

APPENDIX C: INTEGRALS

The integrals appearing in Eq. (3.16), apart from their overall factors, are expressed in terms of the modified Bessel functions

$$\int dz e^{-z^2/2} (\dots) = e^{-q^2/4} \sqrt{\frac{\pi}{2}} [c_0 I_0(q^2/4) + c_1 I_1(q^2/4)] \quad (\text{C1})$$

with coefficients

$$\begin{aligned}
(c_0, c_1) &= (1/4)(2 + q^2, -q^2) \text{ for } \xi_q, \\
(c_0, c_1) &= (1/2)(q^2, -2 - q^2) \text{ for } \lambda_q, \\
(c_0, c_1) &= (q^2/16)(-2 + q^2, -q^2) \text{ for } b_q, \\
(c_0, c_1) &= -(q/8)(1 + q^2, -3 - q^2) \text{ for } \tau_q. \quad (\text{C2})
\end{aligned}$$

-
- ¹K. S. Novoselov, A. K. Geim, S. V. Morozov, D. Jiang, M. I. Katsnelson, I. V. Grigorieva, S. V. Dubonos, and A. A. Firsov, *Nature (London)* **438**, 197 (2005).
- ²Y. Zhang, Y.-W. Tan, H. L. Stormer, and P. Kim, *Nature (London)* **438**, 201 (2005).
- ³Y. Zhang, Z. Jiang, J. P. Small, M. S. Purewal, Y.-W. Tan, M. Fazlollahi, J. D. Chudow, J. A. Jaszczak, H. L. Stormer, and P. Kim, *Phys. Rev. Lett.* **96**, 136806 (2006).
- ⁴N. H. Shon and T. Ando, *J. Phys. Soc. Jpn.* **67**, 2421 (1998); Y. Zheng and T. Ando, *Phys. Rev. B* **65**, 245420 (2002).
- ⁵V. P. Gusynin and S. G. Sharapov, *Phys. Rev. Lett.* **95**, 146801 (2005).
- ⁶N. M. R. Peres, F. Guinea, and A. H. Castro Neto, *Phys. Rev. B* **73**, 125411 (2006).
- ⁷K. Nomura and A. H. MacDonald, *Phys. Rev. Lett.* **96**, 256602 (2006); see also, for a related gap-opening mechanism, E. V. Gorbar, V. P. Gusynin, V. A. Miransky, and I. A. Shovkovy, *Phys. Rev. B* **78**, 085437 (2008).
- ⁸J. Alicea and M. P. A. Fisher, *Phys. Rev. B* **74**, 075422 (2006).
- ⁹M. I. Katsnelson, K. S. Novoselov, and A. K. Geim, *Nat. Phys.* **2**, 620 (2006).
- ¹⁰R. Jackiw and C. Rebbi, *Phys. Rev. D* **13**, 3398 (1976); A. N. Redlich, *Phys. Rev. Lett.* **52**, 18 (1984); R. Jackiw, *Phys. Rev. D* **29**, 2375 (1984).
- ¹¹A. J. Niemi and G. W. Semenoff, *Phys. Rev. Lett.* **51**, 2077 (1983).
- ¹²G. W. Semenoff, *Phys. Rev. Lett.* **53**, 2449 (1984).
- ¹³F. D. M. Haldane, *Phys. Rev. Lett.* **61**, 2015 (1988).
- ¹⁴N. Fumita and K. Shizuya, *Phys. Rev. D* **49**, 4277 (1994).
- ¹⁵K. S. Novoselov, E. McCann, S. V. Morozov, V. I. Fal'ko, M. I. Katsnelson, U. Zeitler, D. Jiang, F. Schedin, and A. K. Geim, *Nat. Phys.* **2**, 177 (2006).
- ¹⁶E. McCann and V. I. Fal'ko, *Phys. Rev. Lett.* **96**, 086805 (2006).
- ¹⁷M. Koshino and T. Ando, *Phys. Rev. B* **73**, 245403 (2006).
- ¹⁸T. Ohta, A. Bostwick, T. Seyller, K. Horn, and E. Rotenberg, *Science* **313**, 951 (2006).
- ¹⁹E. McCann, *Phys. Rev. B* **74**, 161403(R) (2006).
- ²⁰E. V. Castro, K. S. Novoselov, S. V. Morozov, N. M. R. Peres, J. M. B. Lopes dos Santos, J. Nilsson, F. Guinea, A. K. Geim, and A. H. Castro Neto, *Phys. Rev. Lett.* **99**, 216802 (2007).
- ²¹H. Min, B. Sahu, S. K. Banerjee, and A. H. MacDonald, *Phys. Rev. B* **75**, 155115 (2007).
- ²²J. B. Oostinga, H. B. Heersche, X. Liu, A. F. Morpurgo, and L. M. K. Vandersypen, *Nature Mater.* **7**, 151 (2008).
- ²³The dielectric response of graphene is quite unusual even in the absence of a magnetic field. See, T. Ando, *J. Phys. Soc. Jpn.* **75**, 074716 (2006); E. H. Hwang and S. Das Sarma, *Phys. Rev. B* **75**, 205418 (2007); B. Wunsch, T. Stauber, F. Sols, and F. Guinea, *New J. Phys.* **8**, 318 (2006).
- ²⁴K. Shizuya, *Phys. Rev. B* **75**, 245417 (2007); **77**, 075419 (2008).

- (2008).
- ²⁵T. Misumi and K. Shizuya, Phys. Rev. B **77**, 195423 (2008).
- ²⁶Y. Barlas, R. Côté, K. Nomura, and A. H. MacDonald, Phys. Rev. Lett. **101**, 097601 (2008).
- ²⁷Cyclotron resonances in bilayer graphene are also discussed by D. S. L. Abergel and V. I. Fal'ko, Phys. Rev. B **75**, 155430 (2007); D. S. L. Abergel and T. Chakraborty, Phys. Rev. Lett. **102**, 056807 (2009).
- ²⁸L. M. Malard, J. Nilsson, D. C. Elias, J. C. Brant, F. Plentz, E. S. Alves, A. H. Castro Neto, and M. A. Pimenta, Phys. Rev. B **76**, 201401(R) (2007).
- ²⁹S. M. Girvin, A. H. MacDonald, and P. M. Platzman, Phys. Rev. B **33**, 2481 (1986).
- ³⁰K. Moon, H. Mori, K. Yang, S. M. Girvin, A. H. MacDonald, L. Zheng, D. Yoshioka, and S.-C. Zhang, Phys. Rev. B **51**, 5138 (1995).
- ³¹To recover the ϕ degree of freedom one may simply replace (Ω^1, Ω^2) with $\Omega'^1 = \Omega^1 \cos \phi + \hat{\Omega}^2 \sin \phi$ and $\Omega'^2 = -\Omega^1 \sin \phi + \Omega^2 \cos \phi$ and rotate (p_y, p_x) analogously.
- ³²K. Shizuya, Int. J. Mod. Phys. B **17**, 5875 (2003).
- ³³C. Kallin and B. I. Halperin, Phys. Rev. B **30**, 5655 (1984).
- ³⁴With only the effect of vacuum polarization, calculated in Ref. [25](#), is taken into account, one finds $\epsilon_{sc} \approx 9, 3.6, 2.8,$ and 2.5 for $B[T]=1, 10, 20,$ and $30,$ respectively.
- ³⁵E. A. Henriksen, Z. Jiang, L.-C. Tung, M. E. Schwartz, M. Takita, Y.-J. Wang, P. Kim, and H. L. Stormer, Phys. Rev. Lett. **100**, 087403 (2008).